ACS Catalysis

Viewpoint

Cite This: ACS Catal. 2019, 9, 1985−1992

pubs.acs.org/acscatalysis

Analogy between Enzyme and Nanoparticle Catalysis: A Single-Molecule Perspective

Rong Ye,[†] Xianwen Mao,[†] Xiangcheng Sun, and Peng Chen*

Department of Chemistry and Chemical Biology, Cornell University, Ithaca, New York 14853, United States

1. INTRODUCTION

Catalysis as a field is classically divided into three areas: homogeneous, heterogeneous, and biological catalysis.[1] For the latter two (i.e., biological catalysis and heterogeneous catalysis), their dissimilarity can be apparent intuitively, from the scenes of fruit fermentation in a rural winery to make wine and oil refining in a process plant to produce gasoline. In addition to the practical differences, technological terms common in both areas show divergences in meaning. A highly relevant example is the term turnover number.[2] It refers to the maximum number of substrate molecules converted to products per enzyme molecule per second, often written as k_{cat} in enzyme catalysis; while the same term means the number of moles of reactants that a mole of catalyst converts before deactivation, usually abbreviated as TON in heterogeneous catalysis.

However, the development of characterization tools provides increasingly deeper insights into these catalytic systems, revealing their intrinsic resemblances. One evident yet important similarity is the size of these catalysts. The size of a typical enzyme molecule, the key component of biological catalysts, ranges from a few to ∼10 nm, while the active components of most heterogeneous catalysts are nanoparticles (NPs) with sizes of about a few to hundreds of nanometers.[3] Interestingly, the nanometer sizes of enzymes and NPs (i.e., hundreds or more atoms per enzyme or NP) are often associated with heterogeneity among individual enzymes or NPs, leading to disorder (vide infra).[4] Therefore, some catalytic behaviors of individual enzymes or NPs are often hidden from ensemble-averaged measurements.[5] Yet, because of the small sizes of enzymes and NPs, measurements at the single-enzyme or single-particle level remain difficult, if not impossible, until the recent advent of single-molecule techniques.[6−12] In this Viewpoint, we discuss the analogies between enzyme and NP catalysis based on selected recent studies of single-molecule enzyme and NP catalysis. Specifically, we focus on comparing reaction kinetics, static disorder, dynamic disorder, parallel reaction pathways, and allosteric effects between enzyme and NP catalysis at the single-molecule level. In the discussions of NPs, we mainly refer to metallic NPs, but we will cite selective references about other types of materials, such as semiconductors, layered double hydroxides, and zeolites, at the appropriate sections.

2. REACTION KINETICS

The Michaelis−Menten (MM) model successfully describes the kinetic behavior of most biocatalysts. This model involves an enzyme E, binding to a substrate S, to form a complex ES that transforms into another complex EP, which in turn quickly releases the product P and regenerates the original enzyme E (Figure 1A). The MM mechanism has the following approximations. First, the rate-limiting step of the catalysis is

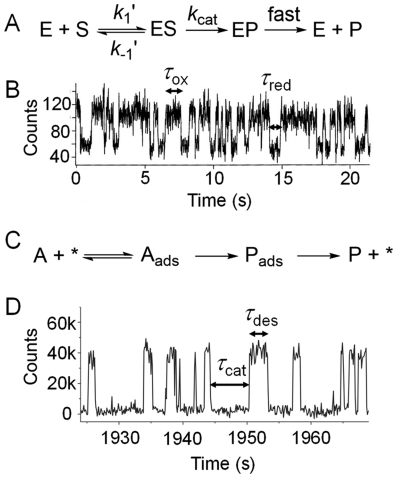

Figure 1. The basis of single-molecule enzyme and NP catalysis. (A,C) Elementary steps of the MM model for enzyme catalysis (A) and the simplified LH model for NP catalysis (C). (B) Real-time observation of enzymatic turnovers of a single cholesterol oxidase enzyme molecule catalyzing the oxidation of cholesterol molecules. The emission exhibits stochastic blinking behaviors as the enzyme active site toggles between oxidized (fluorescent) and reduced (nonfluorescent) states, each on−off cycle corresponding to an enzymatic turnover. τ_{ox} or τ_{red} represents the waiting time on the oxidized or reduced state, respectively. Adapted with permission from ref 13. Copyright 1998 American Association for the Advancement of Science. (D) A segment of the fluorescence trajectory from a single NP in a movie of single-turnover detection of single-Au-nanoparticle catalysis, where the reduction of the nonfluorescent resazurin by NH_2OH is catalyzed to generate the fluorescent resorufin. τ_{cat} or τ_{des} represents the waiting time of a catalytic turnover or a product desorption event, respectively. Adapted with permission from ref 14. Copyright 2008 Nature Publishing Group.

the reaction from ES to EP. Second, quasi-equilibrium of the complex ES with E and S is established; that is, $k_{cat} \ll k_{-1}'$. Third, the release of the product P is fast compared with the catalytic conversion rate. Under steady-state approximation, the rate of product formation is given by

$$v = \frac{v_{max}[S]}{[S] + K_M} \quad (1)$$

Received: December 10, 2018
Published: January 22, 2019

DOI: 10.1021/acscatal.8b04926
ACS Catal. 2019, 9, 1985−1992

where [S] is the substrate concentration in equilibrium, K_M (= $(k_{cat} + k_{-1}')/k_1'$) is the MM constant and has the unit of concentration, and v_{max} (= $k_{cat}[E]_T$) is the maximum reaction rate and $[E]_T$ is the total enzyme concentration.

Xie and colleagues contributed the first report of single-molecule enzymatic kinetics in 1998.[13] From the emission intensity trajectory of an enzyme cholesterol oxidase that contains a fluorescent cofactor at its active site, they achieved the real-time observation of single turnovers between its oxidized (fluorescent) and reduced (nonfluorescent) states (Figure 1B). The individual waiting times on the oxidized and reduced states are stochastic, but their average values, $\langle\tau_{ox}\rangle$ and $\langle\tau_{red}\rangle$, respectively, correspond to the inverse of the reaction rate. Using such methods to analyze the waiting times from the single-molecule study of the enzyme β-galactosidase in catalyzing the generation of a fluorescent product resorufin, Xie and colleagues revisited the MM kinetics in a single-molecule context in their seminal work in 2006.[15] They concluded that single-molecule enzyme catalysis shows saturation kinetics that are similar to the ensemble measurements (Figure 2A), but a single-molecule MM equation is

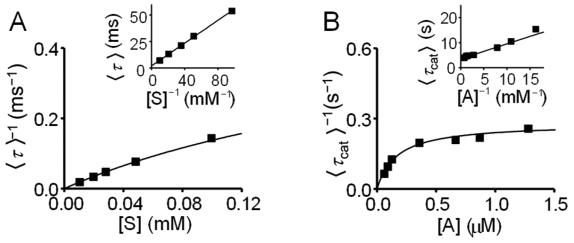

Figure 2. Representative kinetics plots of single-molecule enzyme and NP catalysis. (A) Dependence of $\langle\tau\rangle^{-1}$ on the substrate concentration [S] for single β-galactosidase molecules in catalyzing the hydrolysis of resorufin-β-D-galactopyranoside to generate a fluorescent resorufin product. Inset: the corresponding single-molecule Lineweaver–Burke plot, $\langle\tau\rangle$ versus $[S]^{-1}$. Adapted with permission from ref 15. Copyright 2006 Nature Publishing Group. (B) Dependence of $\langle\tau_{cat}\rangle^{-1}$ on the reactant concentration [A] for single Au nanoparticles in catalyzing the conversion of resazurin to the fluorescent resorufin. Inset: the corresponding single-molecule Lineweaver–Burke plot, $\langle\tau_{cat}\rangle$ versus $[A]^{-1}$. Adapted with permission from ref 14. Copyright 2008 Nature Publishing Group.

given to emphasize the different microscopic interpretations compared with the conventional one:

$$\langle\tau\rangle^{-1} = \frac{k_{cat}[S]}{[S] + K_M} \tag{2}$$

where τ is the waiting time before each product generation. Considering that $v_{max} = k_{cat}[E]_T$, where k_{cat} is the turnover number defined in the Introduction section and $[E]_T$ is the total concentration of enzyme molecules, dividing both sides of Equation 1 by $[E]_T$, that is, evaluating the rate per enzyme, renders it equivalent to Equation 2. However, despite the ever-fluctuating conformations of single enzymes (to be discussed in Section 4), the turnover number k_{cat}, and K_M that is dependent on k_{cat}, in the single-enzyme MM equation are the weighted harmonic means for all conformers—this is the essential microscopic interpretation of the single-enzyme MM equation.

On the other hand, NP catalysis can often be described by the Langmuir–Hinshelwood (LH) kinetics model for heterogeneous catalysis. It has the following assumptions. First, the rate-limiting step of the catalysis is the reaction between two surface-adsorbed reactant molecules. Second, quasi-equilibrium of reactant adsorption is established, and the adsorption follows the Langmuir adsorption model. Third, desorption of the product P is fast compared with the catalytic reaction rate. The classical LH model was developed for bimolecular reactions. However, when the two reactants adsorb to different types of surface sites (i.e., noncompetitive adsorption) and the concentration of one reactant is held constant, the elementary kinetic steps involved are comparable to the MM model. In this case, a reactant A binds to a surface site *, forming an adsorbed species A_{ads} that transforms into the adsorbed product P_{ads}, which in turn quickly releases the product P and regenerates a surface site * (Figure 1C).

Chen and colleagues published the first report of the real-time observation of single turnovers on a single NP catalyst, using gold NPs as a model catalytic system, in 2008.[14] From the emission intensity trajectory of a fluorescent product resorufin, produced from the gold NP catalyzed reduction of resazurin by hydroxylamine, the real-time single-turnover detection of single-particle catalysis was accomplished (Figure 1D). Similarly, the waiting times between and during these stochastic fluorescence bursts, τ_{cat} and τ_{des}, respectively, can be used to analyze the reaction kinetics. Averaging over many events, the product formation rate $\langle\tau_{cat}\rangle^{-1}$ exhibits saturation kinetics (Figure 2B). The [A] dependence of $\langle\tau_{cat}\rangle^{-1}$ follows the single-molecule LH equation:

$$\langle\tau_{cat}\rangle^{-1} = \frac{\gamma_{eff}K_1[A]}{1 + K_1[A]} \tag{3}$$

where K_1 is the reactant adsorption equilibrium constant and has the unit of inverse concentration, and γ_{eff} represents the combined reactivity of all surface catalytic sites on one NP.

Inspecting Figure 2A,B, one can see that the reaction rate varies linearly with the substrate or reactant concentration [S] or [A] (i.e., pseudo first-order kinetics) when $[S] \ll K_M$ or $[A] \ll 1/K_1$, i.e., when the concentration term in the denominator in eq1 or 2 is negligible. However, when [S] or [A] becomes large enough to dominate the denominator, the reaction rate is independent of the substrate/reactant concentration and the reaction exhibits zero-order kinetics because all the enzymes or surface sites are occupied under these conditions. The plateau reaction rate depends on the reactivity of each active site as well as the number of available enzyme sites (i.e., monomer or oligomer) or surface sites. The analogous saturation kinetics between enzyme catalysis and NP catalysis are attributable to the similarity in the formalism of the two single-molecule equations. Rewriting eqs1 and 2 to the reciprocal form for the conventional Lineweaver–Burke plot, both $\langle\tau\rangle$-vs-$[S]^{-1}$ and $\langle\tau_{cat}\rangle$-vs-$[A]^{-1}$ follow a linear relation (insets of Figure 2A,B).

In addition to Xie's group, single-molecule enzyme kinetics was also investigated by Szabo,[16,17] Walt,[18] Noji,[19] Yan,[20] Walter,[21] and Moerner[22] et al. on a myriad of systems. Notably, the release and binding kinetics of inhibitors were probed at a single-enzyme level by Walt and colleagues.[23] On the other hand, via single-particle catalysis studies, Chen and colleagues further identified the LH kinetics on spherical Au NPs of different sizes,[24] Au nanorods,[25,26] and bimetallic nanostructures,[27,28] as well as the competitive LH kinetics on Au nanoplates[29] and Pt NPs.[30] In addition, Tachikawa and co-workers reported the photocatalytic LH kinetics on semiconductor TiO_2 NPs,[5,31,32] Weckhuysen et al. reported LH

DOI: 10.1021/acscatal.8b04926
ACS Catal. 2019, 9, 1985−1992

kinetics on zeolite H-ZSM-5 crystals,[33] Fang et al. discussed LH kinetics on spatially confined multilayer nanocatalysts,[34] and Xu and colleagues observed the LH kinetics on a variety of nanocatalysts.[35−39]

3. STATIC DISORDER

Disorder, either static or dynamic, is a ubiquitous phenomenon in enzyme and heterogeneous catalysis.[4] Static disorder refers to the static heterogeneity of reactivity among individual enzyme molecules or catalyst particles. Static disorder is to be distinguished from dynamic disorder, which is the fluctuation of reactivity of a single enzyme or particle over time, which will be discussed in the next section.

Static disorder is often masked in ensemble measurements, but it is directly observable in single-enzyme or single-particle measurements. As their names suggest, single-enzyme or single-particle studies disclose the catalytic behavior of individual enzymes or particles, so comparisons among different individuals become straightforward. Static disorder can be aptly revealed by the distribution of kinetic parameters that are independent of substrate/reactant concentration and time, namely, k_{cat} for enzymes and γ_{eff} for NPs, each value of which can be obtained from analyzing the distribution of microscopic waiting times obtained from the fluorescence intensity trajectories such as those in Figure 1B,D (Figure 3A,B). A broad distribution of k_{cat} or γ_{eff} unambiguously verifies the static disorder of enzymes or NPs, respectively (Figure 3A,B insets).

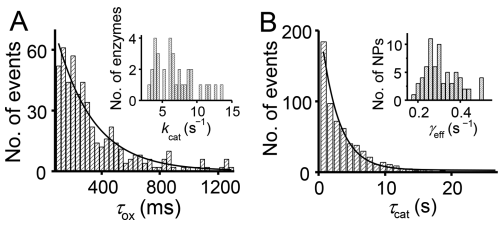

Figure 3. Distributions of kinetic parameters confirm the static disorder of single-molecule enzyme and NP catalysis. (A) Distribution of τ_{ox} derived from one fluorescence turnover trajectory as in Figure 1B, in which k_{cat} is the rate-limiting step for the enzymatic reaction. Solid line: an exponential fit where the exponential decay rate corresponds to k_{cat}. Inset: distribution of k_{cat} from many enzyme molecules in the same sample. Each value of k_{cat} is time-averaged over each entire trajectory. Adapted with permission from ref 13. Copyright 1998 American Association for the Advancement of Science. (B) Distribution of τ_{cat} derived from one fluorescence turnover trajectory of a single Au NP as in Figure 1D. Solid line: an exponential fit where the exponential decay rate corresponds to γ_{eff}. Inset: distribution of γ_{eff} from many NPs in the same sample. Each value of γ_{eff} is time-averaged over each entire trajectory. Adapted with permission from ref 40. Copyright 2009 Royal Society of Chemistry.

The causes of static disorder of enzyme and NPs are highly analogous. As the structures of catalysts govern their intrinsic catalytic properties, static disorder implies the heterogeneity of the structures among individual enzymes/NPs. Unlike common small-molecule organometallic compounds (typical homogeneous catalysts), whose molecular structures can often be precisely replicated and well maintained, enzymes and NPs are susceptible to variations in their structure during the expression or synthesis, and storage. Specifically, post-translational modifications[41] and proteolytic damages[13] such as oxidation of the key residues are postulated for the static disorder of electrophoretically pure enzymes. As for NPs, the dispersity of the size and shape is well-known, due to the distinctions of nucleation and growth history among different particles.[42] Chen and colleagues even identified a gradient of reactivity from the center to the edge along a nanorod[25] or nanoplate[29] (i.e., static disorder at the subparticle level) likely stemming from a gradient of the surface defect density caused by different growth rates from the center to the edge of the same NP. Static disorder is also observed in nanomaterials beyond metallic NP catalysts (e.g., layered double hydroxides,[43] carbon nanotubes,[44] semiconductors,[36,45] and synthetic zeolites).[46−48]

4. DYNAMIC DISORDER

While static disorder compares the properties of individual catalysts with one another at the same time, dynamic disorder is about the temporal fluctuations of the rate of one catalyst at a time scale comparable to or longer than a turnover cycle.[49,50] The coexistence of both static and dynamic disorder usually leads to broad distributions of molecular properties of an ensemble. Because of its nonsynchronous nature, dynamic disorder is extremely challenging to be probed and to be deconvoluted from static disorder, using ensemble-averaged experiments, and it is beyond the scope of conventional chemical kinetics.[13] It is directly accessible from single-molecule turnover trajectories, however.

Dynamic disorder often manifests itself as a memory effect of a single enzyme or NP; e.g., for catalytic kinetics, a turnover is dependent on its previous turnovers. Thus, dynamic disorder is best demonstrated by the autocorrelation function of the microscopic waiting time τ of catalytic turnovers $C_\tau(m)$, namely, the correlation of an event (i.e., waiting time τ) with a delayed copy of itself as a function of delay in the units of turnover index m along the single-molecule turnover trajectories. For both turnover trajectories of the single enzyme and single NP in Figure 1B,D, their $C_\tau(m)$ show clear exponential decay behaviors (Figure 4A,B). The exponential decay time constants give the corresponding underlying fluctuation correlation times, i.e., the memory times of the dynamic disorder.

The physical origins of the dynamic disorder in enzymes and NPs are conceptually equivalent. Enzymatic rate fluctuations originate from the slow conformational fluctuations of the enzyme molecule (Figure 4C), which can span a time scale of 10^{-3} to 10 s.[15,51−53] Analogously, dynamic disorder of NPs is ascribed to dynamic surface restructuring, which is supported by the increased fluctuation rates (i.e., inverse of the fluctuation correlation time) at increasing rates of turnovers, due to the catalysis-induced surface restructuring (Figure 4D).[14] Note that temporal dynamics of NPs is only relevant for small NPs, whose fluctuation time scales are comparable to the characteristic time scales of catalytic kinetics. When NPs are large, such fluctuations become too slow to be relevant to the catalysis. Chen and colleagues have further shown that the time scale of dynamic disorder of NPs depends on the sizes[24] and the chemical composition (Pt vs Au)[30] of NPs; both observations are consistent with a well-known fact that the surface restructuring dynamics depend on the surface energy of NPs, which is strongly influenced by their size and composition. Relatedly, Xu and colleagues discussed the dynamic disorder of Pd NPs[39] and a small molecule trapped in porous hollow SiO_2 nanospheres,[54] and the effects of temperature on dynamic disorder.[37]

DOI: 10.1021/acscatal.8b04926
ACS Catal. 2019, 9, 1985−1992

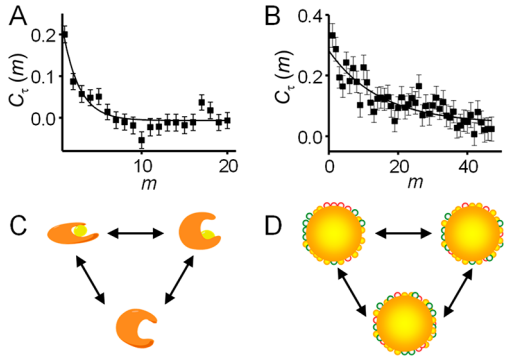

Figure 4. Dynamic disorder of enzyme and NP catalysis revealed via single-molecule turnover trajectory analyses.(A) The autocorrelation function of τ_{ox}, i.e., $C_\tau(m)$, as a function of the turnover index m, derived from a single cholesterol oxidase turnover trajectory as in Figure 1B. Solid line: single exponential fit with a decay constant of 1.6 ± 0.5 turnovers. With the averaged turnover cycle of 600 ms, a correlation time of 1.0 ± 0.3 s is obtained for the fluctuating k_{cat} of this enzyme. Adapted with permission from ref 13. Copyright 1998 American Association for the Advancement of Science. (B) The autocorrelation function of τ_{cat} (i.e., $C_\tau(m)$) as a function of the turnover index m, derived from one turnover trajectory of a single Au NP. Solid line: single exponential fit with a decay constant of 12.5 ± 2.9 turnovers. With the averaged turnover time of ∼4.5 s for this trajectory, a correlation time of ∼56 s is obtained for the fluctuating γ_{eff} of this NP. Adapted with permission from ref 14. Copyright 2008 Nature Publishing Group. (C) Schematic illustration of the fluctuations of conformations of a single enzyme molecule. (D) Schematic illustration of dynamic surface restructuring of a single NP. Different colors represent surface atoms having different local structural arrangements.

5. MULTIPLE REACTION PATHWAYS

Owing to the ubiquitous presence of static and dynamic disorder in enzymes and NPs, as detailed in Sections 3 and 4, both systems are prone to exhibit multiple reaction pathways. For example, conformational changes in enzymes can be associated with different product releasing pathways,[55] while the intrinsic structural heterogeneity of NPs makes them display varying catalytic mechanisms among individual catalyst particles,[14] or even among the different sites on a single particle.[14,24] It is a challenge to elucidate complicated reaction pathways, including in ensemble measurements which average out the hidden structural variations of enzyme molecules and NPs, and the different transient species from different reaction pathways. The single-molecule approach enjoys unique advantages here in interrogating individual enzymes or NPs and, as a result, could provide a powerful means of unravelling possible parallel reaction pathways.

Lu and co-workers have reported a study on the conformational dynamics of a common monomeric enzyme with a heme prosthetic group, horseradish peroxidase (HRP), and its catalytic mechanisms toward a fluorogenic reaction (oxidation of nonfluorescent amplex red to fluorescent resorufin), by combining single-molecule photon time-stamping spectroscopy and magnetic tweezers that impose a controlled mechanical force on a single enzyme.[55] Two distinct conformational states of HRP were identified during the time when the product molecule resorufin is released from the enzyme active site (Figure 5A, top): (i) a tightly bound state that confines the product molecule within the enzyme catalytic pocket possibly due to strong electrostatic interactions and other interactions between the product molecule and the enzyme, and (ii) a loosely bound state that corresponds to the opening up of the enzyme active site in order to release the product molecule to the surrounding solution. Under an external piconewton pulling force on the enzyme, the product-releasing pathway is dominated by that associated with the loosely bound state of the active site (Figure 5A, bottom). This finding is of broad relevance in enzymatic catalysis since the conformational dynamics of enzymes has been shown to have pronounced effects on reaction kinetics.[13,15,52,56,57] More relatedly, the formation of transient, intermediate conformational states in enzymes has been experimentally observed during the product releasing step of enzymatic catalysis.[58,59]

With regard to NP catalysis, using a single-molecule catalysis imaging technique, Chen and colleagues[14] have shown that, due to their structural heterogeneity, individual Au NPs exhibit distinct kinetic mechanisms during catalysis of a fluorogenic probe reaction (reduction of weakly fluorescent resazurin to

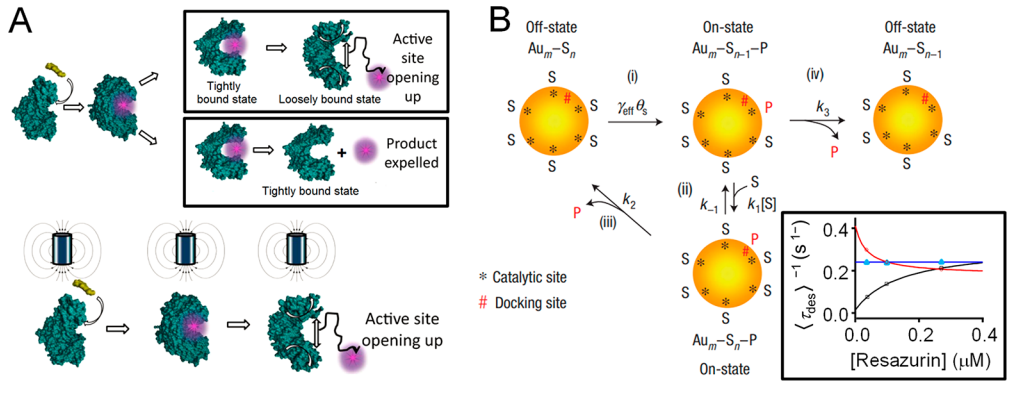

Figure 5. The presence of multiple reaction pathways in single-enzyme and single-nanoparticle catalysis. (A) Schematic illustration of the product-releasing pathways for HRP-catalyzed oxidation of amplex red to resorufin without (top panel) and with (bottom panel) external mechanical perturbation using magnetic tweezers that generate a piconewton pulling force to the enzyme. Purple sphere: product molecule resorufin. Adapted with permission from ref 55. Copyright 2016 National Academy of Science. (B) Schematic diagram of the kinetic mechanism of Au NP-catalyzed reduction of resazurin to resorufin. Au_m: Au NP. S: resazurin. P: resorufin. Au_m-S_n indicates a Au NP with n adsorbed resazurin molecules. On-state and off-state indicate the fluorescence state at each reaction stage. Inset: three different types of resazurin concentration dependence of $\langle\tau_{des}\rangle^{-1}$, from three single Au NPs of type-I (black), type-II (red), and type-III (blue). Adapted with permission from ref 14. Copyright 2008 Nature Publishing Group.

DOI: 10.1021/acscatal.8b04926
ACS Catal. 2019, 9, 1985−1992

fluorescent resorufin) (Figure 5B). Three different types of reactant concentration [A] dependences of the product dissociation rate, $\langle \tau_{des} \rangle^{-1}$, were observed (Figure 5B, inset), and can be described by eq 4:

$$\langle \tau_{des} \rangle^{-1} = \frac{k_2 K_2[A] + k_3}{1 + K_2[A]} \quad (4)$$

Due to the existence of two distinct product dissociation pathways on Au NPs, as shown in Figure 5B, the product dissociate rate may display three different kinetic behaviors: (I) asymptotically increasing with [A] if $k_2 > k_3$, (II) asymptotically decreasing with [A] if $k_2 < k_3$, and (III) remaining constant at any [A] if $k_2 = k_3$ or $K_2 = 0$. The three different behaviors differ in relative magnitudes of the two rate constants, reflecting the heterogeneity in selectivity of individual particles in these two parallel product dissociation pathways. Another work by the Chen group uncovered the size-dependent selectivity toward the product dissociation reaction during Au NP catalysis,[24] further highlighting the utility of in situ single-molecule catalysis approaches in probing fundamental reaction mechanisms and offering definitive evidence of possible parallel reaction pathways. Such heterogeneity in reaction kinetics and mechanisms, likely due to variations in NP surface structures, has also been observed through the use of single-molecule catalysis approach for a range of other NP systems under various catalysis conditions, offering additional insights into several factors affecting NP catalytic mechanisms and reaction pathways, such as molecular diffusion,[60] the type of surface crystal facets,[38,39] and the presence of a kinetic compensation effect.[37]

6. CATALYSIS COOPERATIVITY BETWEEN SPATIALLY DISTINCT SITES

Allostery is a phenomenon in which the binding of a molecule or the occurrence of a reaction at an active site of a macromolecule affects the binding or reaction at another site of some distance away. Such a phenomenon indicates a cooperative communication over distances, and is well documented for biological systems or processes, such as enzymatic catalysis, protein functions, and DNA−protein interactions.[61] In general, allostery is a distinguishing feature for enzymes and proteins, due to a well-known behavior of these biomacromolecules that they often undergo significant conformational changes upon binding of a small molecule or a ligand.

The majority of the works that examine allosteric effects were carried out at the ensemble level. For instance, one classical approach in enzymatic catalysis is to study the relation between the reaction rate and the substrate concentration, and a sigmoidal one implies catalytic allostery. Ensemble-level studies, however, do not contain any spatial information and thus cannot provide knowledge of spatial correlation of molecular binding or reactions, which allostery is all about. Single-molecule approaches, which can offer direct spatial information, are hence well-suited to probe allosteric effects.

Xie and colleagues reported a single-molecule study of allostery in DNA−protein interactions, and provided clear experimental evidence that the dissociation rate of a DNA-bound protein is affected by the binding of another protein at a distant site.[61] For example, they found that the dissociation rate of a DNA-bound protein GRDBD (i.e., a DNA binding domain of glucocorticoid receptor) exhibited a pronounced oscillatory pattern as a function of the number of base pairs (L) between this protein binding site and a distant binding site for another protein (Figure 6), where the oscillation

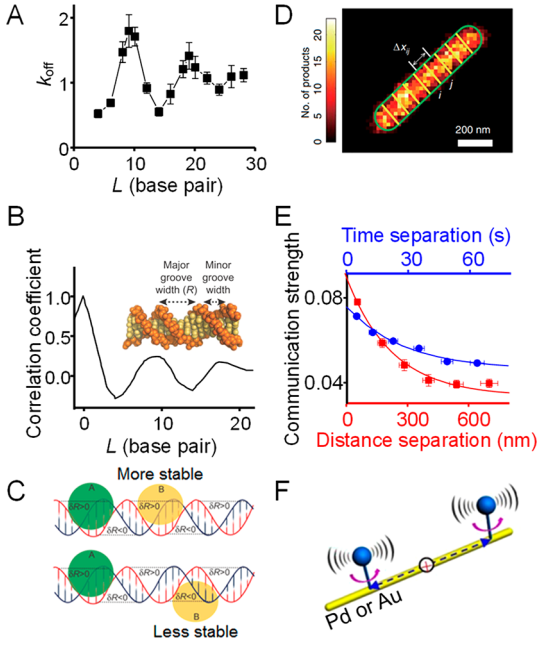

Figure 6. Single-molecule studies of cooperative communication over distances in both biological and nonbiological systems. (A) Normalized dissociation rate constant (k_{off}) of a DNA-bound protein GRDBD as a function of the distance (L) (i.e., the number of base pairs) between the binding site of this protein and the binding site of another protein. (B) MD simulation-derived correlation coefficient of the DNA major groove width (R, see inset) at two locations as a function of the distance (i.e., the number of base pairs) between them. (C) Schematic illustration of the allosteric coupling between two DNA-bound proteins A and B. Panels A−C are adapted with permission from ref 61. Copyright 2013 American Association of the Advancement of Science. (D) Dissection of a super-resolution catalysis image of a mesoporous silica-coated Pd nanorod into ∼100 nm segments. Green line: structural contour of the nanorod determined from scanning electron microscopy. (E) Catalytic communication strength within a single Pd nanorod as a function of the intraparticle distance separation or the time separation between temporally subsequent product-generation events. (F) Schematic illustration of the intraparticle catalytic communication mechanism due to the presence of positively charged messenger species. Panels D−F are adapted with permission from ref 62. Copyright 2018 Nature Publishing Group.

periodicity is about 10 base pairs. Such allostery through a DNA molecule is induced by distortion of its major groove. Using molecular dynamics simulations, the authors showed that the spatial correlation between the major groove widths (R) (Figure 6B inset) at two different locations as a function of their separation displays an oscillatory pattern with a periodicity of about 10 base pairs (Figure 6B), consistent with that observed in the kinetic measurements (Figure 6A). The allosteric coupling between two DNA-binding proteins A and B can be more clearly illustrated in Figure 6C. Assuming that protein B widens R, it would prefer to bind at a location that is already widened by protein A, instead of a location that is narrowed.

Whether such allosteric effects are also present for nonbiological systems has remained unclear, until a recent

DOI: 10.1021/acscatal.8b04926
ACS Catal. 2019, 9, 1985−1992

report by Chen and co-workers showing that nonbiological nanocatalysts, indeed, exhibit such cooperative effects, which are phenomenologically similar to catalytic allostery in enzymes.[62] Leveraging the power of spatiotemporally resolved single-molecule catalysis imaging, these authors have demonstrated that the catalytic reactions on a single nanocatalyst are positively correlated with each other over a distance of hundreds of nanometers and with a temporal memory of about 10 to 100 s. Spatial mapping of the fluorescent product molecules on individual Pd nanorods, one of the nanocatalysts examined in this study, allows for dissecting each nanorod into different, spatially distinct segments (Figure 6D). Moreover, the temporal sequence of the product generation events can be extracted from each segment. A striking discovery is that the strength, quantified through a single event-pair correlation analysis, of intraparticle catalytic communication starts with a clear positive value, and decays exponentially when the intraparticle distance separation or the time separation between temporally subsequent product-generation events increases (Figure 6E). Such trends indicate that a fast reaction at one segment tends to be followed by another fast reaction nearby, resulting in a positive cooperativity between these reactions. In other words, the reactions within a single nanocatalyst indeed communicate with each other.

While phenomenologically it resembles allostery in enzymatic catalysis, such cooperativity in NP catalysis stems from a mechanism distinct from that of biological systems (i.e., conformational perturbation of an enzyme induced by binding of a molecule at a distant location). The intraparticle catalytic communication for the nanocatalysts investigated in this study was identified to originate from the migration of positively charged messenger species, likely a surface hole (e.g., a positive charge localized on metal-oxide species) (Figure 6F), while other plausible causes such as reaction heat dissipation, surface restructuring dynamics, and surface plasmon resonance (for the case of Au catalysts) have been ruled out by control experiments or simulations.

7. CONCLUDING REMARKS

We have provided a discussion of the conceptual analogy between enzyme and NP catalysis from a single-molecule perspective. The kinetic model and the resultant equations have similar forms. Due to intrinsic structural heterogeneity and time-dependent structural dynamics in enzymes or NPs, both catalytic systems involve static and dynamic disorder, and, as a result, exhibit complex reaction mechanisms that are often characterized by multiple parallel reaction pathways. More notably, catalysis cooperativity, which has been long known to be a distinguishing characteristic in enzymatic catalysis, also exists in NP catalysis; yet such cooperative effects in NP catalysis stem from a different mechanism from that in enzymatic catalysis. Single-molecule fluorescence spectroscopy is indeed a powerful approach to revealing the intrinsic properties of enzyme and NP catalysis.

AUTHOR INFORMATION

Corresponding Author

*E-mail: pc252@cornell.edu.

ORCID

Rong Ye: 0000-0002-4171-5964

Peng Chen: 0000-0001-8582-7661

Author Contributions

[†]R.Y. and X.M. contributed equally.

Notes

The authors declare no competing financial interest.

ACKNOWLEDGMENTS

We thank the support by the Department of Energy, Office of Science, Basic Energy Sciences, Catalysis Science Program, under Award DE-SC0004911; and Army Research Office under award W911NF-17-1-0590. R.Y. acknowledges the Cornell Presidential Postdoctoral Fellowship for financial support.

REFERENCES

(1) Ye, R.; Zhao, J.; Wickemeyer, B. B.; Toste, F. D.; Somorjai, G. A. Foundations and strategies of the construction of hybrid catalysts for optimized performances. *Nat. Catal.* **2018**, *1*, 318−325.

(2) Coming together. *Nat. Catal.* **2018**, *1*, 307−307.

(3) Ye, R.; Hurlburt, T. J.; Sabyrov, K.; Alayoglu, S.; Somorjai, G. A. Molecular catalysis science: Perspective on unifying the fields of catalysis. *Proc. Natl. Acad. Sci. U. S. A.* **2016**, *113*, 5159−5166.

(4) Wang, A.; Li, J.; Zhang, T. Heterogeneous single-atom catalysis. *Nat. Rev. Chem.* **2018**, *2*, 65−81.

(5) Hesari, M.; Mao, X.; Chen, P. Charge Carrier Activity on Single-Particle Photo(electro)catalysts: Toward Function in Solar Energy Conversion. *J. Am. Chem. Soc.* **2018**, *140*, 6729−6740.

(6) Betzig, E.; Chichester, R. J. Single Molecules Observed by Near-Field Scanning Optical Microscopy. *Science* **1993**, *262*, 1422−1425.

(7) Moerner, W. E.; Fromm, D. P. Methods of single-molecule fluorescence spectroscopy and microscopy. *Rev. Sci. Instrum.* **2003**, *74*, 3597−3619.

(8) Hell, S. W. Toward fluorescence nanoscopy. *Nat. Biotechnol.* **2003**, *21*, 1347−1355.

(9) Zhuang, X.; Bartley, L. E.; Babcock, H. P.; Russell, R.; Ha, T.; Herschlag, D.; Chu, S. A Single-Molecule Study of RNA Catalysis and Folding. *Science* **2000**, *288*, 2048−2051.

(10) Joo, C.; Balci, H.; Ishitsuka, Y.; Buranachai, C.; Ha, T. Advances in Single-Molecule Fluorescence Methods for Molecular Biology. *Annu. Rev. Biochem.* **2008**, *77*, 51−76.

(11) Benitez, J. J.; Keller, A. M.; Huffman, D. L.; Yatsunyk, L. A.; Rosenzweig, A. C.; Chen, P. Relating dynamic protein interactions of metallochaperones with metal transfer at the single-molecule level. *Faraday Discuss.* **2011**, *148*, 71−82.

(12) Chen, P.; Zhou, X.; Andoy, N. M.; Han, K.-S.; Choudhary, E.; Zou, N.; Chen, G.; Shen, H. Spatiotemporal catalytic dynamics within single nanocatalysts revealed by single-molecule microscopy. *Chem. Soc. Rev.* **2014**, *43*, 1107−1117.

(13) Lu, H. P.; Xun, L.; Xie, X. S. Single-Molecule Enzymatic Dynamics. *Science* **1998**, *282*, 1877−1882.

(14) Xu, W.; Kong, J. S.; Yeh, Y.-T. E.; Chen, P. Single-molecule nanocatalysis reveals heterogeneous reaction pathways and catalytic dynamics. *Nat. Mater.* **2008**, *7*, 992−996.

(15) English, B. P.; Min, W.; van Oijen, A. M.; Lee, K. T.; Luo, G.; Sun, H.; Cherayil, B. J.; Kou, S. C.; Xie, X. S. Ever-fluctuating single enzyme molecules: Michaelis-Menten equation revisited. *Nat. Chem. Biol.* **2006**, *2*, 87−94.

(16) Gopich, I. V.; Szabo, A. Theory of the statistics of kinetic transitions with application to single-molecule enzyme catalysis. *J. Chem. Phys.* **2006**, *124*, 154712.

(17) Min, W.; Gopich, I. V.; English, B. P.; Kou, S. C.; Xie, X. S.; Szabo, A. When Does the Michaelis−Menten Equation Hold for Fluctuating Enzymes? *J. Phys. Chem. B* **2006**, *110*, 20093−20097.

(18) Rissin, D. M.; Gorris, H. H.; Walt, D. R. Distinct and Long-Lived Activity States of Single Enzyme Molecules. *J. Am. Chem. Soc.* **2008**, *130*, 5349−5353.

DOI: 10.1021/acscatal.8b04926
ACS Catal. 2019, 9, 1985−1992

(19) Sakakihara, S.; Araki, S.; Iino, R.; Noji, H. A single-molecule enzymatic assay in a directly accessible femtoliter droplet array. *Lab Chip* **2010**, *10*, 3355−3362.
(20) Zhao, Z.; Fu, J.; Dhakal, S.; Johnson-Buck, A.; Liu, M.; Zhang, T.; Woodbury, N. W.; Liu, Y.; Walter, N. G.; Yan, H. Nanocaged enzymes with enhanced catalytic activity and increased stability against protease digestion. *Nat. Commun.* **2016**, *7*, 10619.
(21) Ditzler, M. A.; Alemán, E. A.; Rueda, D.; Walter, N. G. Focus on function: Single molecule RNA enzymology. *Biopolymers* **2007**, *87*, 302−316.
(22) Goldsmith, R. H.; Tabares, L. C.; Kostrz, D.; Dennison, C.; Aartsma, T. J.; Canters, G. W.; Moerner, W. E. Redox cycling and kinetic analysis of single molecules of solution-phase nitrite reductase. *Proc. Natl. Acad. Sci. U. S. A.* **2011**, *108*, 17269−17274.
(23) Gorris, H. H.; Rissin, D. M.; Walt, D. R. Stochastic inhibitor release and binding from single-enzyme molecules. *Proc. Natl. Acad. Sci. U. S. A.* **2007**, *104*, 17680−17685.
(24) Zhou, X.; Xu, W.; Liu, G.; Panda, D.; Chen, P. Size-Dependent Catalytic Activity and Dynamics of Gold Nanoparticles at the Single-Molecule Level. *J. Am. Chem. Soc.* **2010**, *132*, 138−146.
(25) Zhou, X.; Andoy, N. M.; Liu, G.; Choudhary, E.; Han, K.-S.; Shen, H.; Chen, P. Quantitative super-resolution imaging uncovers reactivity patterns on single nanocatalysts. *Nat. Nanotechnol.* **2012**, *7*, 237−241.
(26) Shen, H.; Zhou, X.; Zou, N.; Chen, P. Single-Molecule Kinetics Reveals a Hidden Surface Reaction Intermediate in Single-Nanoparticle Catalysis. *J. Phys. Chem. C* **2014**, *118*, 26902−26911.
(27) Chen, G.; Zou, N.; Chen, B.; Sambur, J. B.; Choudhary, E.; Chen, P. Bimetallic Effect of Single Nanocatalysts Visualized by Super-Resolution Catalysis Imaging. *ACS Cent. Sci.* **2017**, *3*, 1189−1197.
(28) Zou, N.; Chen, G.; Mao, X.; Shen, H.; Choudhary, E.; Zhou, X.; Chen, P. Imaging Catalytic Hotspots on Single Plasmonic Nanostructures via Correlated Super-Resolution and Electron Microscopy. *ACS Nano* **2018**, *12*, 5570−5579.
(29) Andoy, N. M.; Zhou, X.; Choudhary, E.; Shen, H.; Liu, G.; Chen, P. Single-Molecule Catalysis Mapping Quantifies Site-Specific Activity and Uncovers Radial Activity Gradient on Single 2D Nanocrystals. *J. Am. Chem. Soc.* **2013**, *135*, 1845−1852.
(30) Han, K. S.; Liu, G.; Zhou, X.; Medina, R. E.; Chen, P. How Does a Single Pt Nanocatalyst Behave in Two Different Reactions? A Single-Molecule Study. *Nano Lett.* **2012**, *12*, 1253−1259.
(31) Tachikawa, T.; Yamashita, S.; Majima, T. Evidence for Crystal-Face-Dependent TiO2 Photocatalysis from Single-Molecule Imaging and Kinetic Analysis. *J. Am. Chem. Soc.* **2011**, *133*, 7197−7204.
(32) Tachikawa, T.; Yonezawa, T.; Majima, T. Super-Resolution Mapping of Reactive Sites on Titania-Based Nanoparticles with Water-Soluble Fluorogenic Probes. *ACS Nano* **2013**, *7*, 263−275.
(33) Ristanović, Z.; Hofmann, J. P.; De Cremer, G.; Kubarev, A. V.; Rohnke, M.; Meirer, F.; Hofkens, J.; Roeffaers, M. B. J.; Weckhuysen, B. M. Quantitative 3D Fluorescence Imaging of Single Catalytic Turnovers Reveals Spatiotemporal Gradients in Reactivity of Zeolite H-ZSM-5 Crystals upon Steaming. *J. Am. Chem. Soc.* **2015**, *137*, 6559−6568.
(34) Dong, B.; Pei, Y.; Zhao, F.; Goh, T. W.; Qi, Z.; Xiao, C.; Chen, K.; Huang, W.; Fang, N. In situ quantitative single-molecule study of dynamic catalytic processes in nanoconfinement. *Nat. Catal.* **2018**, *1*, 135−140.
(35) Chen, T.; Dong, B.; Chen, K.; Zhao, F.; Cheng, X.; Ma, C.; Lee, S.; Zhang, P.; Kang, S. H.; Ha, J. W.; Xu, W.; Fang, N. Optical Super-Resolution Imaging of Surface Reactions. *Chem. Rev.* **2017**, *117*, 7510−7537.
(36) Xu, W.; Jain, P. K.; Beberwyck, B. J.; Alivisatos, A. P. Probing Redox Photocatalysis of Trapped Electrons and Holes on Single Sb-doped Titania Nanorod Surfaces. *J. Am. Chem. Soc.* **2012**, *134*, 3946−3949.
(37) Chen, T.; Zhang, Y.; Xu, W. Single-Molecule Nanocatalysis Reveals Catalytic Activation Energy of Single Nanocatalysts. *J. Am. Chem. Soc.* **2016**, *138*, 12414−12421.
(38) Chen, T.; Chen, S.; Zhang, Y.; Qi, Y.; Zhao, Y.; Xu, W.; Zeng, J. Catalytic Kinetics of Different Types of Surface Atoms on Shaped Pd Nanocrystals. *Angew. Chem., Int. Ed.* **2016**, *55*, 1839−1843.
(39) Chen, T.; Chen, S.; Song, P.; Zhang, Y.; Su, H.; Xu, W.; Zeng, J. Single-Molecule Nanocatalysis Reveals Facet-Dependent Catalytic Kinetics and Dynamics of Pallidium Nanoparticles. *ACS Catal.* **2017**, *7*, 2967−2972.
(40) Xu, W.; Kong, J. S.; Chen, P. Probing the catalytic activity and heterogeneity of Au-nanoparticles at the single-molecule level. *Phys. Chem. Chem. Phys.* **2009**, *11*, 2767−2778.
(41) Craig, D. B.; Arriaga, E. A.; Wong, J. C. Y.; Lu, H.; Dovichi, N. J. Studies on Single Alkaline Phosphatase Molecules: Reaction Rate and Activation Energy of a Reaction Catalyzed by a Single Molecule and the Effect of Thermal DenaturationThe Death of an Enzyme. *J. Am. Chem. Soc.* **1996**, *118*, 5245−5253.
(42) Somorjai, G. A.; Li, Y. *Introduction to Surface Chemistry and Catalysis*; John Wiley & Sons, 2010.
(43) Roeffaers, M. B. J.; Sels, B. F.; Uji-i, H.; De Schryver, F. C.; Jacobs, P. A.; De Vos, D. E.; Hofkens, J. Spatially resolved observation of crystal-face-dependent catalysis by single turnover counting. *Nature* **2006**, *439*, 572.
(44) Xu, W.; Shen, H.; Kim, Y. J.; Zhou, X.; Liu, G.; Park, J.; Chen, P. Single-Molecule Electrocatalysis by Single-Walled Carbon Nanotubes. *Nano Lett.* **2009**, *9*, 3968−3973.
(45) Naito, K.; Tachikawa, T.; Fujitsuka, M.; Majima, T. Single-Molecule Observation of Photocatalytic Reaction in TiO2 Nanotube: Importance of Molecular Transport through Porous Structures. *J. Am. Chem. Soc.* **2009**, *131*, 934−936.
(46) Roeffaers, M. B. J.; De Cremer, G.; Libeert, J.; Ameloot, R.; Dedecker, P.; Bons, A.-J.; Bückins, M.; Martens, J. A.; Sels, B. F.; De Vos, D. E.; Hofkens, J. Super-Resolution Reactivity Mapping of Nanostructured Catalyst Particles. *Angew. Chem., Int. Ed.* **2009**, *48*, 9285−9289.
(47) De Cremer, G.; Roeffaers, M. B. J.; Bartholomeeusen, E.; Lin, K.; Dedecker, P.; Pescarmona, P. P.; Jacobs, P. A.; De Vos, D. E.; Hofkens, J.; Sels, B. F. High-Resolution Single-Turnover Mapping Reveals Intraparticle Diffusion Limitation in Ti-MCM-41-Catalyzed Epoxidation. *Angew. Chem., Int. Ed.* **2010**, *49*, 908−911.
(48) De Cremer, G.; Sels, B. F.; De Vos, D. E.; Hofkens, J.; Roeffaers, M. B. J. Fluorescence micro(spectro)scopy as a tool to study catalytic materials in action. *Chem. Soc. Rev.* **2010**, *39*, 4703−4717.
(49) van Oijen, A. M.; Blainey, P. C.; Crampton, D. J.; Richardson, C. C.; Ellenberger, T.; Xie, X. S. Single-Molecule Kinetics of λ Exonuclease Reveal Base Dependence and Dynamic Disorder. *Science* **2003**, *301*, 1235−1238.
(50) Zwanzig, R. Rate processes with dynamical disorder. *Acc. Chem. Res.* **1990**, *23*, 148−152.
(51) De Cremer, G.; Roeffaers, M. B. J.; Baruah, M.; Sliwa, M.; Sels, B. F.; Hofkens, J.; De Vos, D. E. Dynamic Disorder and Stepwise Deactivation in a Chymotrypsin Catalyzed Hydrolysis Reaction. *J. Am. Chem. Soc.* **2007**, *129*, 15458−15459.
(52) Edman, L.; Földes-Papp, Z.; Wennmalm, S.; Rigler, R. The fluctuating enzyme: a single molecule approach. *Chem. Phys.* **1999**, *247*, 11−22.
(53) Hassler, K.; Rigler, P.; Blom, H.; Rigler, R.; Widengren, J.; Lasser, T. Dynamic disorder in horseradish peroxidase observed with total internal reflection fluorescence correlation spectroscopy. *Opt. Express* **2007**, *15*, 5366−5375.
(54) Zhang, Y.; Song, P.; Fu, Q.; Ruan, M.; Xu, W. Single-molecule chemical reaction reveals molecular reaction kinetics and dynamics. *Nat. Commun.* **2014**, *5*, 4238.
(55) Pal, N.; Wu, M. L.; Lu, H. P. Probing conformational dynamics of an enzymatic active site by an in situ single fluorogenic probe under piconewton force manipulation. *Proc. Natl. Acad. Sci. U. S. A.* **2016**, *113*, 15006−15011.
(56) Benkovic, S. J.; Hammes, G. G.; Hammes-Schiffer, S. Free-energy landscape of enzyme catalysis. *Biochemistry* **2008**, *47*, 3317−3321.

DOI: 10.1021/acscatal.8b04926
ACS Catal. 2019, 9, 1985−1992

(57) Henzler-Wildman, K. A.; Thai, V.; Lei, M.; Ott, M.; Wolf-Watz, M.; Fenn, T.; Pozharski, E.; Wilson, M. A.; Petsko, G. A.; Karplus, M.; Hubner, C. G.; Kern, D. Intrinsic motions along an enzymatic reaction trajectory. *Nature* **2007**, *450*, 838−844.
(58) De Simone, A.; Aprile, F. A.; Dhulesia, A.; Dobson, C. M.; Vendruscolo, M. Structure of a low-population intermediate state in the release of an enzyme product. *eLife* **2015**, *4*, No. e02777.
(59) Oyen, D.; Fenwick, R. B.; Stanfield, R. L.; Dyson, H. J.; Wright, P. E. Cofactor-Mediated Conformational Dynamics Promote Product Release From Escherichia coli Dihydrofolate Reductase via an Allosteric Pathway. *J. Am. Chem. Soc.* **2015**, *137*, 9459−9468.
(60) De Cremer, G.; Roeffaers, M. B. J.; Bartholomeeusen, E.; Lin, K. F.; Dedecker, P.; Pescarmona, P. P.; Jacobs, P. A.; De Vos, D. E.; Hofkens, J.; Sels, B. F. High-Resolution Single-Turnover Mapping Reveals Intraparticle Diffusion Limitation in Ti-MCM-41-Catalyzed Epoxidation. *Angew. Chem., Int. Ed.* **2010**, *49*, 908−911.
(61) Kim, S.; Brostromer, E.; Xing, D.; Jin, J. S.; Chong, S. S.; Ge, H.; Wang, S. Y.; Gu, C.; Yang, L. J.; Gao, Y. Q.; Su, X. D.; Sun, Y. J.; Xie, X. S. Probing Allostery Through DNA. *Science* **2013**, *339*, 816−819.
(62) Zou, N. M.; Zhou, X. C.; Chen, G. Q.; Andoy, N. M.; Jung, W.; Liu, G. K.; Chen, P. Cooperative communication within and between single nanocatalysts. *Nat. Chem.* **2018**, *10*, 607−614.

DOI: 10.1021/acscatal.8b04926
ACS Catal. 2019, 9, 1985−1992